Morphological and structural features of the Cd$_x$Pb$_{1-x}$S films obtained by CBD from ethylenediamine-citrate bath

A.D. Kutyavina[a,*] , L.N. Maskaeva[a,b], V.I. Voronin[c],
I.A. Anokhina[d], V.F. Markov[a,b]

a: Ural Federal University named after the first President of Russia B.N. Yeltsin,
   620002, 19 Mira st., Yekaterinburg, Russia
b: Ural Institute of the State Fire Service of the EMERCOM of Russia,
   620062, 22 Mira st., Yekaterinburg, Russia
c: M.N. Miheev Institute of Metal Physics, Ural Branch of Russian Academy of Sciences,
   620108, 18 S. Kovalevskaya st., Yekaterinburg, Russia
d: Institute of High Temperature Electrochemistry, Ural Branch of the Russian Academy of Sciences,
   620990, 20 Akademicheskaya st., Yekaterinburg, Russia
* Corresponding author: n-kutyavina@mail.ru

This article belongs to the regular issue.

Abstract

The calculating of ionic equilibria in the system «Pb(CH$_3$COO)$_2$ – CdCl$_2$ – Na$_3$C$_6$H$_5$O$_7$ – (NH$_3$)$_2$(CH$_2$)$_2$ – N$_2$H$_4$CS» allowed us to find conditions and concentration regions of PbS and CdS co-deposition. The determined conditions provided the CBD obtaining of Cd$_x$Pb$_{1-x}$S ($0 \le x \le 0.033$) substitutional solid solutions films with a cubic structure B1 (space group $Fm\overline{3}m$) with the grains preferred orientation (200). We established the evolution of the surface morphology of the synthesized films from cubic crystallites to hierarchical structure of globular aggregates by scanning electron microscopy. A quantitative analysis of diffraction patterns showed a decrease of microstrains in Cd$_x$Pb$_{1-x}$S films by a about factor of 3 with an increase of the cadmium chloride concentration in the reaction mixture from 0.005 to 0.14 mol/l. The excess of the cadmium content, established by EDX analysis, in the studied films as compared to its content in the solid solution is associated with the additional formation of the amorphous CdS phase up to 72 mol %.

1. Introduction

Ternary compounds in the CdS-PbS system, f.e. the Cd$_x$Pb$_{1-x}$S substitutional solid solutions, have been attracting interest among the researchers of semiconductor structures for half a century. The possibility of regulating the band gap from small of PbS (0.4 eV) to rather big of CdS (2.42 eV) value finds application in the production of heterojunctions and solar cells based on these substances [1-2]. The Cd$_x$Pb$_{1-x}$S photosensitivity in the range of 0.4-3.1 μm is used to create IR detectors [3-4]. The developed morphology of the layer surface facilitates using these thin-film compounds as sensitive elements for the determination of toxic compounds in gas and liquid media [5]. Various nanoscale structures are constructed on the basis of Cd$_x$Pb$_{1-x}$S solid solutions, in particular, quantum dots, nanocrystals, and nanowires [6-8].

The thin-film Cd$_x$Pb$_{1-x}$S solid solutions have the unique functional physical and chemical properties. Semiconductor or ionic conductivity, mechanical, thermal, and radiation resistance of these compounds can be controlled by changing the cadmium content or particle sizes making up the film. Also, we can note relative simplicity of their preparation. Many researchers prefer chemical deposition from aqueous solutions (chemical bath deposition, CBD) [1-5,8-20]. This method allows obtaining Cd$_x$Pb$_{1-x}$S solid solutions both in powder and thin-film states on substrates of any nature and configuration without complex technological equipment.

The chemical bath deposition essence of semiconductor compounds is the interaction of metal cations and S^{2-} anions in solution. The sources of those ions are the metal salt and chalcogenizer, respectively. Ligands allow regulating the amount of free metal ions in the reactor due to

the gradual dissociation of complex compounds. Consequently, the rate of solid phase formation reduces leading to form a film structure. In situ control the morphology, composition, structure, and semiconducting properties of $Cd_xPb_{1-x}S$ is possible by varying the components concentrations in the reaction mixture and the deposition conditions (pH of the medium, temperature and duration of synthesis) [9-11], as well as by using different substrates [12].

A typical reaction mixture for the $Cd_xPb_{1-x}S$ solid solutions production by CBD includes lead and cadmium salts, mainly $Pb(CH_3COO)_2$, $Pb(NO_3)_2$ and $CdCl_2$; thiourea $(NH_2)_2CS$ and various alkaline agents: sodium hydroxide NaOH, aqueous ammonia solution NH_4OH, ethylenediamine $(NH_2)_2(CH_2)_2$.

As for the ligand, different research groups use various substances as complexing agents: triethanolamine $(C_6H_{15}NO_3)$, aqueous ammonia (NH_4OH), ethylenediamine $(C_2H_8N_2)$, sodium citrate $(Na_3C_6H_5O_7)$, or a combination thereof. It should be noted that ligands play a key role in the nucleation and growth of a new phase and directly affect the properties of the resulting layers. In a number of works it is quite popular to use either triethanolamine together with an alkaline agent NaOH [13] or an aqueous solution of ammonia [1,17-19], or their combination [10,17,19]. However, the instability of triethanolamine complexes with both lead and cadmium promotes the rapid transformation of these metal ions into sulfide and the aggregation of sulfide particles in the bulk of the solution. Solid phase precipitates at the reactor bottom in the powder form, reducing the thickness of the $Cd_xPb_{1-x}S$ layer.

The use of an ammonia aqueous solution as a complex agent [14] leads to formation of a film surface consisting of spherical particles of ~50 nm. Their shape is further transformed into a plate-like one with increase in the cadmium salt content in the bath. Since ammonia forms stable complexes only with cadmium, in the system under consideration OH^- ions act as ligand for Pb^{2+} ions. The instability constant of the $Pb(OH)_4^{2-}$ tetradentate complex ($pk_{1-4,in}$ = 16.3 [19]) significantly exceeds the values of the $Cd(NH_3)_n^{2-}$ complexes instability constants ($pk_{1-4,in}$ = 6.56 [19]). As a result, free cadmium ions prevail in the solution, which leads to the enrichment of the synthesized layers with Cd. Thin-film $Cd_xPb_{1-x}S$ structures (x = 0.35; 0.42; 0.49) synthesized by the authors of [2] had a crystal lattice period of 6.0295–6.0227 Å. That value is more typical of the wurtzite type CdS hexagonal modification ($B4$, space group $P6_3mc$). Attempts to obtain the compositions $Cd_{0.2}Pb_{0.8}S$ and $Cd_{0.4}Pb_{0.6}S$ in [15] and [16] led to the formation of CdS films with PbS inclusions.

Similar structures consisting of spherical nanoaggregates up to 10 nm were obtained from reaction mixtures containing a mixture of triethanolamine and ammonia as ligands [17, 18]. Note that in these publications the authors did not give the true composition of the solid solution, indicating only the elemental composition of the

compound. However, the thermodynamic assessment of the solid phases PbS and CdS formation [12] showed the possibility of the cadmium cyanamide producing at pH > 10. Impurity phases can negatively affect the properties of the obtained semiconductor layers.

To reduce the rate of metal ions release into the solution, Pentia et al. [4] used the disodium salt of ethylenediaminetetraacetic acid $C_{10}H_{14}N_2Na_2O_8$ (EDTA) in an ammonia alkaline medium. This ligand provides the strong complexes formation of both lead ($Pb(EDTA)^{2-}$ $pk_{1,in}$ = 18.04 [19]) and cadmium ($Cd(EDTA)^{2-}$ $pk_{1,in}$ = 16.46 [19]). As a result, films were obtained consisting of a mixture of cubic and tetrahedral crystallites. The films size particles decreased with an increase in the content of cadmium ions in the reaction bath. Despite the fact that in this work a decrease the studied $Cd_xPb_{1-x}S$ films lattice constant was observed, the authors unreasonably assert that the cadmium content x in the composition of the solid solution can vary in a wide range from 0 to 1 by fitting of the concentration ratio of lead and cadmium salts in a reaction bath.

Researchers [3,7,11,12,20] used a reaction mixture containing simultaneously two complexing agents: an aqueous solution of ammonia and sodium citrate. It was found that the $Cd_xPb_{1-x}S$ solid solutions films deposited from this reaction bath mainly consist of faceted particles whose shape and size depend on the composition [20] and the type of substrate [12]. Nevertheless, in this system there is a possibility of the formation of individual CdS phase [9,12]. The CdS deposition may be associated with the formation of insufficiently stable ammonia complexes of cadmium (the biggest instability constant for the $Cd(NH_3)_4^{2-}$ complex $pk_{1-4,in}$ = 6.56 [19]) Hence, the active Cd^{2+} ions can arrive intensively into the reaction medium.

Ethylenediamine $(NH_3)_2(CH_2)_2$ (En) can be an alternative to aqueous ammonia, because it has weak basic properties for providing an alkaline medium necessary for the hydrolytic thiourea decomposition. Another important advantage of ethylenediamine is its low volatility, which contributes to a constant pH of the reaction mixture. Bearing in mind the disadvantage of using the same ligand for lead and cadmium due to their competition, we have decided to supplement the formulation by ethylenediamine in addition citrate ions, which are effective for creating stable complexes. Ethylenediamine forms strong complexes with both lead ($Pb(En)^{2+}$ ($pk_{1,in}$ = 7.00); $Pb(En)_2^{2+}$ ($pk_{1-2,in}$ = 8.45) [21]), and with cadmium ($Cd(En)^{2+}$ ($pk_{1,in}$ = 5.63), $Cd(En)_2^{2+}$ ($pk_{1-2,in}$ = 10.22), $Cd(En)_3^{2+}$ ($pk_{1-3,in}$ = 12.29) [21]).

The ethylenediamine-citrate mixture has proven well in the preparation of $Cd_xPb_{1-x}S$ solid solutions [9]. However, the authors of the publication used a rather small range of cadmium salt concentrations (up to 0.025 mol/l).

It should be noted that intuitive approaches prevail in the overwhelming majority of publications devoted to the synthesis of $Cd_xPb_{1-x}S$ solid solutions by CBD. An experimental search of the process conditions and of the reac-

tion baths compositions is also often encountered accompanied formal reactions of interaction between precursors. Calculation of the concentration range of the lead and cadmium sulfides formation allows predicting the formation of a solid solution before the start of synthesis. Determination of deposition conditions with the least labor input is one of the important aims of a researcher using CBD.

In this regard, this work is devoted to the ionic equilibria analysis with the determination of the potential area of the $Cd_xPb_{1-x}S$ solid solutions formation in the system «$Pb(CH_3COO)_2 - CdCl_2 - Na_3C_6H_5O_7 - (NH_3)_2(CH_2)_2 - N_2H_4CS$». The goal of this research is deposition of $Cd_xPb_{1-x}S$ thin films using found formation boundary conditions, the study of morphology, composition and crystal structure of these compounds.

2. Experimental

The reaction mixture for the chemical bath deposition of $Cd_xPb_{1-x}S$ solid solutions films included the following components. The precursors were lead acetate $Pb(CH_3COO)_2$ 0.04 mol/l and cadmium chloride $CdCl_2$. The cadmium salt concentration was varied in the range 0.005–0.14 mol/l. Ethylenediamine $(NH_3)_2(CH_2)_2$ (En) 0.6 mol/l and sodium citrate $Na_3C_6H_5O_7$ (Na_3Cit) 0.33 mol/l provided ligands for lead and cadmium ions. Ethylenediamine also served as an alkaline agent, and thiourea $(NH_2)_2CS$ was used as a chalcogenizer. Lead sulfide films were obtained under the same conditions without the cadmium salt in the reaction bath. The films synthesis was carried out on pre-degreased ST-50 sitall substrates in sealed glass reactors (100 ml), which were placed in the TS-TB-10 liquid thermostat heated to 353 K. The process duration was 120 minutes.

The thickness of the films was determined using an interference microscope (Linnik microinterferometer) MII-4M with a measurement error of 20%.

The microstructure and elemental composition of the films were studied using MIRA 3 LMU scanning electron microscope at the electron beam accelerating voltage of 10 kV and a JEOL JSM-5900 LV scanning electron microscope with an EDS Inca Energy 250 energy-dispersive X-ray (EDX) analyzer.

X-ray studies of the deposited films were carried out by a PANalytical Empyrean Series 2 diffractometer in Cu Kα radiation in the parallel beam geometry with a position-sensitive PIXel3D detector providing a resolution on 2Θ scale of at least 0.0016°. The diffraction patterns were recorded in 20–100 degrees (2Θ) range with the step of 0.02°, the scanning time was 10 s at a point.

The structural parameters of the $Cd_xPb_{1-x}S$ films were refined by the full-profile Rietveld analysis [22, 23] using the Fullprof software [24]. To separate the contributions of grain size and deformations in the studied films into the width of the diffraction peaks, the conventional Williamson – Hall plot equation was used [25]:

$$\beta \cdot \cos\Theta = 0.9\lambda/D + 4\varepsilon \cdot \sin\Theta \qquad (1)$$

where D is the average size of the coherent scattering regions, taken as the average particle size, β is the half-width of the peak in radians, λ is the wavelength of the X-ray radiation used, $\varepsilon = \Delta d/d$ is the deformation, d is the interplanar distance.

3. Thermodynamic assessment of the formation boundary conditions of PbS, CdS, Cd(OH)₂ and Pb(OH)₂

To determine the CBD optimal conditions, analysis of ionic equilibria was carried out in the system «$Pb(CH_3COO)_2 - CdCl_2 - Na_3C_6H_5O_7 - (NH_3)_2(CH_2)_2 - N_2H_4CS$» according to the method proposed in [26]. These calculations allowed estimating the formation regions of the main phases (PbS and CdS) and impurities ($Cd(OH)_2$, $Pb(OH)_2$).

The prerequisite for obtaining thin-film metal sulfide is to slow down the rate of the metal salt transformation into sulfide. The rate decreasing is achieved by reducing its active concentration due to the metal ions binding into complex compounds. In the studied system lead ions form complexes with citrate ions $Pb(Cit)^-$ (instability constant, $pk_{1,in} = 4.34$), $Pb(Cit)_2^{4-}$ ($pk_{1-2,in} = 6.08$), $Pb(Cit)_3^{7-}$ ($pk_{1-3,in} = 6.97$) [19], $Pb(OH)(Cit)^{2-}$ ($pk_{1,in} = 13.72$) [21]; with hydroxide ions $Pb(OH)^+$ ($pk_{1,in} = 7.52$), $Pb(OH)_2$ ($pk_{1-2,in} = 10.54$), $Pb(OH)_3^-$ ($pk_{1-3,in} = 13.95$), $Pb(OH)_4^{2-}$ ($pk_{1-4,in} = 16.3$) [19], and also with ethylenediamine $Pb(En)^{2+}$ ($pk_{1,in} = 7.00$); $Pb(En)_2^{2+}$ ($pk_{1-2,in} = 8.45$) [21]. For cadmium, the ligands were ethylenediamine $Cd(En)^{2+}$ ($pk_{1,in} = 5.63$), $Cd(En)_2^{2+}$ ($pk_{1-2,in} = 10.22$), $Cd(En)_3^{2+}$ ($pk_{1-3,in} = 12.29$) [19], citrate ions $Cd(Cit)^-$ ($pk_{1,in} = 5.36$) [19], $Cd(OH)(Cit)^{2-}$ ($pk_{1,in} = 9.3$) [21] and hydroxide ions $Cd(OH)^+$ ($pk_{1,in} = 3.92$), $Cd(OH)_2$ ($pk_{1-2,in} = 7.65$), $Cd(OH)_3^-$ ($pk_{1-3,in} = 8.70$), $Cd(OH)_4^{2-}$ ($pk_{1-4,in} = 8.65$) [19].

The regions of individual lead and cadmium sulfides formation, as well as their co-deposition region, were found as a graphical solution of the equilibrium conditions equation in the coordinates "the of the initial metal salt concentration power pC_{in} – the ligand concentration [$Na_3Cit(En)$] – pH" at 298 K [26]:

$$pC_{in} = pSP_{MS} - p\alpha_{M^{2+}}$$
$$- \left(pk_{H_2S}^{1,2} + \frac{1}{2}pK_{SS} - 2pH + \frac{1}{2}p[CS(NH_2)_2]_{in} + \frac{1}{2}p\frac{\beta_c}{\beta_s} \right) \qquad (2)$$
$$- \frac{0.86 \cdot \sigma \cdot V_M}{R \cdot T \cdot r_{cr}},$$

$$pC_{in} = SP_{M(OH)_2} - p\alpha_{M^{2+}} - 2pK_w + 2pH, \qquad (3)$$

where p is the power (negative logarithm); C_{in} is the lead or cadmium salt initial concentration; $pSP_{MS}, pSP_{M(OH)_2}$ are the solubility products' powers of sulfides CdS ($pSP_{CdS} = 26.6$) and PbS ($pSP_{PbS} = 27.8$) and hydroxides $Cd(OH)_2$ ($pSP_{Cd(OH)_2} = 15.8$) and $Pb(OH)_2$ ($pSP_{Pb(OH)_2} = 13.66$) [19], respectively; $[CS(NH_2)_2]_{in}$ is the thiocarbamide initial concentration in solution, equal to 0.6 mol/l; σ is the specific

surface energy of metal sulfide (σ_{PbS} = 1.2 J/m² and σ_{CdS} = 0.9 J/m²); V_m is the molar volume of the synthesized phase $V_{m(PbS)}$ = 31.9·10⁻⁶ m³/mol and $V_{m(CdS)}$ = 29.97·10⁻⁶ m³/mol; r_{cr} is the critical nucleus radius (3.5·10⁻⁹ m) [26]; R is the ideal gas constant, J/(mol·K); T is the temperature of the process, 298 K; $pk_{H_2S}^{1,2}$ is the hydrogen sulfide dissociation constant, 1.3·10⁻²⁰ [19]; K_{SS} is the thiourea hydrolytic decomposition constant, 3.2·10⁻²³ [27]; β_s and β_c are the values that include the dissociation constants of hydrogen sulfide H_2S and cyanamide H_2CN_2, calculated by the expressions $\beta_s = [H_3O^+]^2 + k_{HS^-}^1[H_3O^+] + k_{H_2S}^{1,2}$, $\beta_c = [H_3O^+]^2 + k_{HCN_2^-}^1[H_3O^+] + k_{H_2CN_2}^{1,2}$, where $k_{HS^-}^1$, $k_{HCN_2^-}^1$ and $k_{H_2S}^{1,2}$, $k_{H_2CN_2}^{1,2}$ are the first stage dissociation constants of hydrogen sulfide and cyanamide ($k_{HS^-}^1$ = 6.99 [19], $k_{HCN_2^-}^1$ = 10.33 [27]) and their cumulative ones ($k_{H_2S}^{1,2}$ = 19.59 [19], $k_{H_2CN_2}^{1,2}$ = 21.51 [27]); $p\alpha_{M^{2+}}$ is the power of the fraction of free lead or cadmium ions in uncomplexed forms. The calculation was carried out considering all possible lead and cadmium forms according to the method proposed in [26]. The last term in Eq. (2) is the derivative of the Thomson - Ostwald relation. This expression determines the supersaturation contribution of lead or cadmium sulfide in the system, taking into account the formation of critical size nuclei.

Sulfide ions formed during the decomposition of thiourea are distributed between the ions of two metals. Hence the $Cd_xPb_{1-x}S$ solid solution formation will occur by way of competing reactions of the CdS and PbS formation. To exclude the limiting effect of the chalcogenizer, the deposition of $Cd_xPb_{1-x}S$ solid solutions was carried out with an excess of thiourea concentration by about 3–13 times compared with the metal concentrations in the reaction mixture.

Thermodynamic assessment of potential regions of the sparingly soluble phases formation in the studying system was performed at a temperature of 298 K under varying the concentration of ethylenediamine (En) from 0.1 to 1.0 mol/l (*a*) and sodium citrate (Na₃Cit) from 0.1 to 0.6 mol/l (*b*) considering the crystallization factor (Fig. 1). The predicted simultaneous deposition area of CdS and PbS solid phases corresponds to the space lying between the surfaces characterizing the initial conditions for the deposition of sulfides (upper surfaces) and hydroxides (lower surfaces) of these metals. In three-dimensional coordinates pC_{in} = f(pH, [L]) the plotted dependences reveal that the CdPbS ternary compound formation without hydroxides admixtures begins with the cadmium sulfide precipitation at pH = 10–14 (*a*) and 10–12 (*b*). In the less alkaline region (pH = 8–10) the process begins with the PbS formation.

The simultaneous deposition area of solid phases of both PbS, CdS sulfides and hydroxides Pb(OH)₂ and Cd(OH)₂ is situated under the concentration planes of the lead and cadmium hydroxides (lower surfaces) formation at pH 11.7–14.0 (*a*) and 11.2–14.0 (*b*). It should be noted that, in the system under discussion, the sulfides formation occurs according to a heterogeneous mechanism by sulfidization of lead and cadmium hydroxides at pH > 11.

The reaction mixture composition was formed from calculations and preliminary experiments. Mirror films with good adhesion to the substrate were obtained with varying the concentration of cadmium salt (0.005–0.14 mol/l). The synthesized films were 400 to 650 nm thick. A change in the gray color (characteristic of PbS) to a dark blue and light green hue (imparted by the content cadmium) indicated the CdPbS three-component compound formation.

4. Results and Discussion

The morphology of PbS films (*a*) and CdPbS thin-film ternary compounds obtained from reaction baths containing 0.01 (*b*) and 0.1 mol/l (*c*) CdCl2 is shown in Fig. 2.
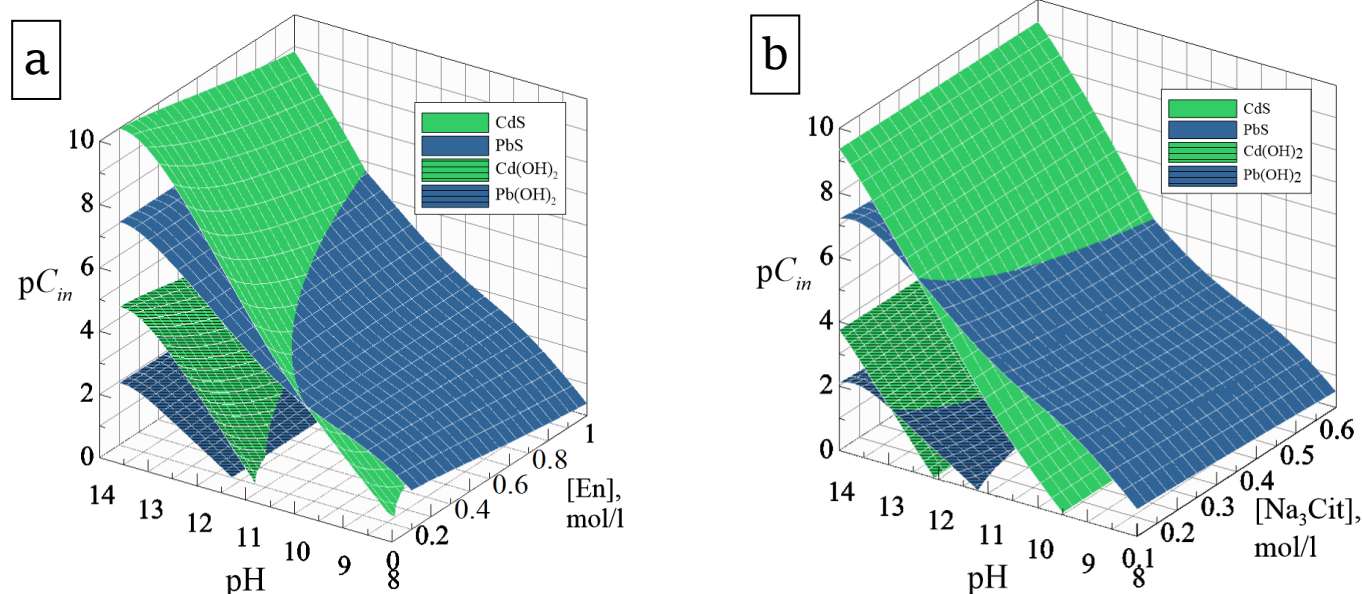

Fig. 1 Boundary conditions of the PbS, CdS, Pb(OH)₂ and Cd(OH)₂ sparingly soluble phases formation depending on the pH of the medium and the concentration of ethylenediamine (En) (*a*) and sodium citrate Na₃Cit (*b*). Calculations were performed at [Na₃Cit] = 0.3 mol/l (*a*) and [En] = 0.6 mol/l (*b*), T = 298 K
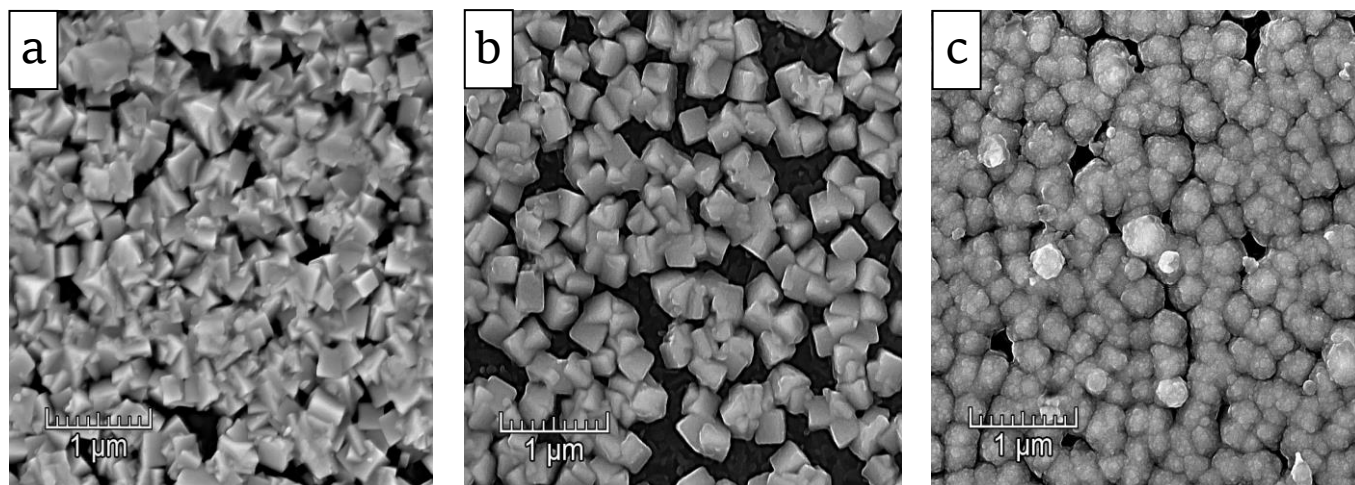
Fig. 2 SEM images of PbS (a) and CdPbS films obtained from reaction baths containing (b) 0.01 and (c) 0.1 mol/l CdCl₂

The lead sulfide film analysis revealed that the average observed crystallite size was ~150–200 nm, and the film continuity degree did not exceed ~80% (Fig. 2*a*). The minimum cadmium salt amount introduction (0.01 mol/l) into reactor led to a slowdown in the rate of formation of lead sulfide, which was also noted by the authors in [28], and the formation of a uniform film consisting of cubic crystallites with an edge of ~150 nm. The particles did not completely cover the substrate surface (Fig. 2*b*). The cubic grains shape is due to the presence in the system of sufficiently stable ethylenediamine complexes of lead. The destruction of these complexes requires additional energy, which increases the energy barrier of interaction between lead and thiourea ions. According to [29], the process proceeds in a thermodynamic regime, the crystallites grows along the <111> directions.

The radical change in the CdPbS films morphology has occurred with the 0.1 mol/l cadmium chloride introduction into the reaction mixture. The obtained films grains composed of the spherical globules ~300–400 nm in size, representing clusters of nanoparticles 50–70 nm in size (Fig. 2*c*). The presence of the hierarchical structure characteristic of CdS [30] is a consequence of the block deposition mechanism implementation. In the bulk of the reaction mixture, solid phase clusters form followed by deposition on the substrate surface [31].

The crystal structure of solid solution films deposited from solutions with 0.005, 0.01, 0.1, 0.12, and 0.14 mol/l concentrations of cadmium chloride was studied by X-ray diffraction. XRD patterns of the synthesized PbS and ternary CdPbS compounds are shown in Fig. 3. The observed peaks corresponded to the PbS cubic structure $B1$ (space group $Fm\bar{3}m$) and to the sitall substrate (TiO₂ and cordierite). The gradual shift of all reflections to the region of greater angles 2Θ evidences solid solutions formation (Fig. 3, inset). As a result, a slight decrease of the period cubic lattice $B1$ is observed from 0.5933(8) to 0.5929(2), 0.5923(6), 0.5918(0), 0.5920(7), and 0.5918(0) nm (Table 1).
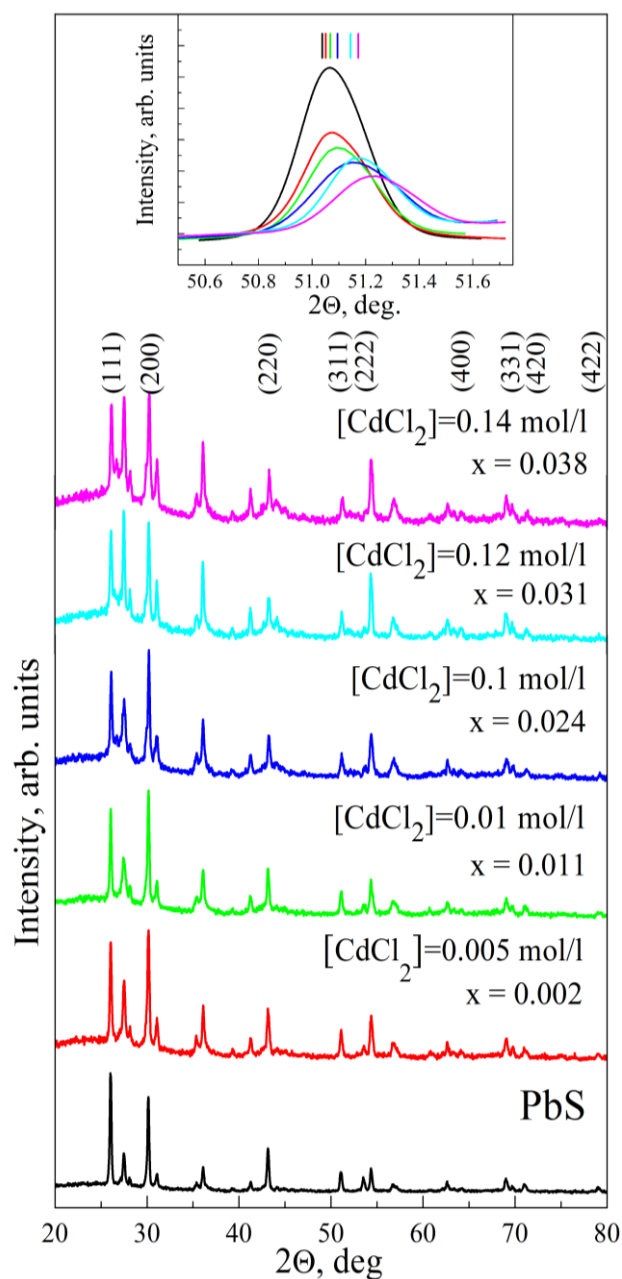

Fig.3 X-ray diffraction patterns of PbS film and Cd$_x$Pb$_{1-x}$S solid solution films obtained at different CdCl₂ contents in the reaction bath. The inset shows the (311) $B1$ peak shift of the Cd$_x$Pb$_{1-x}$S films to 2Θ high-angle region.

The observed crystal lattice period decrease is due to the replacement of lead (II) ions (r = 0.120 nm [32]) by cadmium ions with smaller radius (r = 0.097 nm [32]) in the PbS structure. To estimate the relative content of cadmium and lead, we used the $Cd_xPb_{1-x}S$ (a_{SS}) solid solutions lattice period decreasing (a_{SS}), the experimental value for PbS a_{PbS} = 0.5933(8) nm, and the lattice period for the pseudocubic $B1$ structure a_{CdS}=0.546 nm given in [33–36]. Vegard's rule was used [37-38] to determine the (x) cadmium relative content in $Cd_xPb_{1-x}S$ solid solutions. According to Vegard's rule, the molar fraction of cadmium is defined as $x = (a_{PbS} - a_{SS})/(a_{PbS} - a_{CdS})$.

The performed calculation allowed us to establish the relative content of cadmium x in the lead metal sublattice with an accuracy of ± 0.001 (Table 1). Comparison of the established solid solutions compositions (Table 1) with the PbS - CdS system equilibrium phase diagram [39] indicates a significant supersaturation of the lead sulfide lattice by cadmium for all synthesized $Cd_xPb_{1-x}S$ solid solutions (0 <x ≤ 0.033) at 353 K.

A quantitative analysis of X-ray diffraction patterns was performed by the full-profile analysis method using Fullprof software. The synthesized PbS layers were formed from grains with a predominant orientation (111) with a texture degree T_{111} equal to 35.6% (Table 1). The presence of 0.005 mol/l cadmium salt in the reactor leads to a change in the dominant crystallite growth direction from [111] to [200] (Table 1). The grains reorientation is consistent with the results of scanning electron microscopy (Fig. 2b). The insignificant structure ordering is observed with the $CdCl_2$ concentration rise: the texture coefficient $T_{(200)}$ increases from 22.4 to 28.2%.

The diffraction reflections on the studying films XRD patterns (Fig. 3) were broadened due to the small particle size and the microstrains presence. The separation of the size and deformation contributions to the reflections broadening and the estimation of coherent scattering regions average size, taken in the first approximation as the average grains size (D), was performed using the Williamson-Hall extrapolation method. The estimated microstresses $\Delta d/d$ in $Cd_xPb_{1-x}S$ solid solutions films indicated microstrains decreasing from $11.5 \cdot 10^4$ to $3.5 \cdot 10^4$ with the growth of the cadmium salt concentration in the reaction mixture up to 0.14 mol/l.

The coherent scattering regions size (D) of $Cd_xPb_{1-x}S$ ($x \leq 0.028$) solid solutions films increased from 110 to 123-139 nm with increase in the cadmium chloride content to 0.12 mol/l in comparison with the individual PbS layer, and decreased to 77 nm at 0.14 mol/l of $CdCl_2$.

Local energy-dispersive X-ray spectroscopy (EDX) was carried out to establish the elemental composition of the synthesized films over the entire films surface area in at least 10 points. The results of EDX analysis are given in Table 2. According to the data, the individual PbS film contained (49.7 ± 0.4 at %) lead and (50.3 ± 0.4 at %) sulfur, i.e. there was an excess of chalcogen. In the ternary CdPbS compounds the cadmium content increased from 9.54 to 37.39 at % with an increasing of the cadmium salt concentration in the reaction bath. The ratio between the total content of metals (Cd + Pb) and sulfur S was within 1.0-1.05.

According to the results of EDX analysis, the cadmium content in the synthesized films exceeds the value calculated from the data of X-ray diffraction in the $Cd_xPb_{1-x}S$ solid solution (Table 2). This means that the synthesized

Table 1 The lattice parameter (a), the cadmium content (x) in $Cd_xPb_{1-x}S$ solid solution, portion of the grains with predominant orientation (200) or (111) along substrate plane (T_{200} or T_{111}), the averaged values of microdeformation in the film volume <$\Delta d/d$>, sizes of coherent scattering regions D given for $Cd_xPb_{1-x}S$ thin films obtained with different concentrations of [$CdCl_2$] cadmium chloride in the reaction bath.

| | Content of the cadmium salt in the reaction bath, [$CdCl_2$], mol/l | | | | | |
	0	0.005	0.01	0.1	0.12	0.14
a_{B1} (nm) ±0.00001	0.5933(8)	0.5933(1)	0.5929(2)	0.5923(6)	0.5920(7)	0.5918(0)
x in $Cd_xPb_{1-x}S$	–	0.001	0.010	0.022	0.028	0.033
T_{200} (%)	–	22.5	24.2	24.5	21.8	28.2
T_{111} (%)	35.6	–	–	–	–	–
<$\Delta d/d$>, $\cdot 10^{-4}$	4.8	11.5	6.0	6.2	5.7	3.5
D, nm	110	138	123	139	130	77

Table 2 Effect of the concentration of cadmium chloride on the composition of $Cd_xPb_{1-x}S$ solid solutions. Composition of the reaction mixture, mol/l: [$PbAc_2$] = 0.4, [En] = 0.6, [TM] = 0.6, [Na_3Cit] = 0.3. The temperature of synthesis was 353 K.

| [$CdCl_2$], mol/l | Content of elements in the film, at % | | | Formula composition of the film (without separation into crystalline and amorphous phases) | Formula composition of the $Cd_xPb_{1-x}S$ solid solution, estimation by the lattice parameter, ±0.004 | Phase composition of the film, mol % | |
	Cd ±0.07	Pb ±0.05	S ±0.08			$Cd_xPb_{1-x}S$ solid solution	CdS amorphous sulfide
0.005	9.54	40.45	50.01	$Cd_{0.19}Pb_{0.81}S_{0.99}$	$Cd_{0.001}Pb_{0.999}S$	~81	19
0.01	16.35	34.09	49.56	$Cd_{0.32}Pb_{0.68}S_{1.02}$	$Cd_{0.010}Pb_{0.990}S$	69	31
0.10	34.14	16.77	49.09	$Cd_{0.67}Pb_{0.33}S_{1.04}$	$Cd_{0.022}Pb_{0.978}S$	34	66
0.12	36,79	13,84	49.36	$Cd_{0.73}Pb_{0.27}S_{1.03}$	$Cd_{0.028}Pb_{0.972}S$	28	72
0.14	37.39	13.87	48.74	$Cd_{0.73}Pb_{0.27}S_{1.05}$	$Cd_{0.033}Pb_{0.967}S$	28	72

films contain, in addition to 28–81 mol.% crystalline $Cd_xPb_{1-x}S$, 19–72 mol.% the cadmium sulfide amorphous phase.

The high content of the CdS amorphous phase in the synthesized films was due to the more favorable conditions for CdS formation at the pH of thiourea hydrolytic decomposition (pH = 11-12). That assumption is consistent with the potential thermodynamic area assessment of CdS and PbS sulfides co-precipitation in the system under discussion.

5. Conclusions

The concentration regions of the isovalent lead sulfides PbS and cadmium CdS co-precipitation were determined based on the ionic equilibria analysis in the system «$Pb(CH_3COO)_2$ – $CdCl_2$ – $Na_3C_6H_5O_7$ – $(NH_3)_2(CH_2)_2$ – N_2H_4CS». For the studied system, these calculations allowed defining the deposition parameters of the $Cd_xPb_{1-x}S$ substitutional solid solutions.

Films of supersaturated $Cd_xPb_{1-x}S$ solid solutions with the cadmium content up to x = 0.033 were obtained by chemical bath deposition at 353 K on sitall substrates. The crystalline structure of the films was B1 cubic (space group $Fm\bar{3}m$).

SEM analysis of CdPbS films demonstrated the evolution of the morphology layers. The polycrystalline structure has replaced by globular aggregates with increasing of the cadmium chloride concentration up to 0.14 mol/l in the reaction bath.

The higher cadmium content in the CdPbS films found by EDX analysis in comparison with its amount estimated from the XRD data is associated with the formation of the CdS amorphous phase.

Acknowledgements

References

1. Suryavanshi KE, Dhake RB, Patil AM, Sonawane MR. Growth mechanism and transport properties of chemically deposited Pb Cd S thin film's photoelectrochemical (PEC) solar cell. Optik. 2020;165008. doi:10.1016/j.ijleo.2020.165008

2. Ounissi A, Ouddai N, Achour S. Optical characterisation of chemically deposited $Pb_{(1-x)}Cd_xS$ films and a $Pb_{1-x}Cd_xS(n)/Si(p)$ heterojunction. Eur Phys J Appl Phys. 2007;37(3):241–5. doi:10.1051/epjap:2007034

3. Maskaeva LN, Markov VF, Porkhachev MYu, Mokrousova AO. Thermal and radiation stability IR-detectors based on films of solid solutions $Cd_xPb_{1-x}S$. Pozharovzryvobezopasnost [Fire and Explosion Safety]. 2015;24(9):67-73. Russian. doi:10.18322/PVB.2015.24.09.67-73

4. Pentia E, Draghici V, Sarau G, et al. Structural, electrical, and photoelectrical properties of $Cd_xPb_{1-x}S$ thin films prepared by chemical bath deposition. J Electrochem Soc. 2004;151(11):G729–33. doi:10.1149/1.1800673

5. Bezdetnova AE, Markov VF, Maskaeva LN, et al. Determination of nitrogen dioxide by thin-film chemical sensors based on $Cd_xPb_{1-x}S$. J Anal Chem. 2019;74(12):1256–62. doi:10.1134/S1061934819120025

6. Au GHT, Shih WY, Tseng SJ, Shih WH. Aqueous CdPbS quantum dots for near-infrared imaging. Nanotechnology. 2012;23(27):275601(1-9). doi:10.1088/0957-4484/23/27/275601

7. Tan GL, Liu L, Wu W. Mid-IR band gap engineering of $Cd_xPb_{1-x}S$ nanocrystals by mechanochemical reaction. AIP Advances. 2014;4(6):067107(1-11). doi:10.1063/1.4881878

8. Nichols PL, Liu Z, Yin L, et al. $Cd_xPb_{1-x}S$ alloy nanowires and heterostructures with simultaneous emission in mid-infrared and visible wavelengths. Nano Lett. 2015;15(2):909–16. doi:10.1021/nl503640x

9. Rabinovich E, Wachtel E, Hodes G. Chemical bath deposition of single-phase (Pb,Cd)S solid solutions. Thin Solid Films. 2008;517(2):737–44. doi:10.1016/j.tsf.2008.08.162

10. Barote M, Yadav A, Masumdar E. Effect of deposition parameters on growth and characterization of chemically deposited $Cd_{1-x}Pb_xS$ thin films. Chalcogenide Lett. [Internet]. 2021[cited 2021];8(2):129–38. Available from: https://chalcogen.ro/index.php/journals/chalcogenide-letters/11-cl/126-volume-8-number-2-february-2011

11. Maskaeva, LN, Kutyavina AD, Markov VF, et al. Features of the formation of thin films of supersaturated $Cd_xPb_{1-x}S$ solid solutions by chemical bath deposition. Russ J Gen Chem. 2018;88(2):295–304. doi:10.1134/S1070363218020172

12. Maskaeva LN, Pozdin AV, Markov VF, et al. Effect of the substrate nature on the CdPbS film composition and mechanical stresses at the "film–substrate" interface. Semiconductors. 2020;54:1567–76. doi:10.1134/S1063782620120209

13. Rajathi S, Kirubavathi K, Selvaraju K. Preparation of nanocrystalline Cd-doped PbS thin films and their structural and optical properties. J of Taibah University for Science. 2017;11(6):1296–305. doi:10.1016/j.jtusci.2017.05.001

14. Suryavanshi KE, Dhake RB, Patil AM, Sonawane MR. Growth mechanism and transport properties of chemically deposited PbCdS thin film's photoelectrochemical (PEC) solar cell. Optik. 2020;165008. doi:10.1016/j.ijleo.2020.165008

15. Ahmad SM, Kasim SJ, Latif LA. Effects of thermal annealing on structural and optical properties of nanocrystalline $Cd_xPb_{1-x}S$ thin films prepared by CBD. Jordan Journal of Physics [Internet]. 2016[cited 2021];9(2):113–22. Available from: http://journals.yu.edu.jo/jjp/JJPIssues/Vol9No2pdf2016/7.pdf

16. Suryavanshi KE, Dhake RB, Patil AM, et al. Structural properties of $Pb_xCd_{1-x}S$ thin films prepared by chemical bath deposition technique. Int J Adv Res [Internet]. 2014[cited 2021];2(6):491–3. Available from: http://www.journalijar.com/uploads/926_IJAR-3389.pdf

17. Thangavel S, Ganesan S, Chandramohan S, et al. Band gap engineering in PbS nanostructured thin films from near-infrared down to visible range by in situ Cd-doping. J Alloys Comp. 2010;495(1):234237. doi:10.1016/j.jallcom.2010.01.135

18. Deo SR, Singh AK, Deshmukh L, et al. Studies on structural, morphological and optical behavior of chemically deposited $Cd_{0.5}Pb_{0.5}S$ thin films. Optik. 2015;126(20):2311–17. doi:10.1016/j.ijleo.2015.05.130

19. Lurie YuYu. Spravochnik po analiticheskoy khimii [Analytical chemistry handbook]. Moscow: Khimiya; 1989. 488 p. Russian.

20. Maskaeva LN, Voronin BI, Mostovshchikova EV, et al. Chemical bath deposited $Cd_xPb_{1-x}S$ solid solution films: composition, structure, optical properties. Thin Solid Films. 2021;718(12):138468. doi:10.1016/j.tsf.2020.138468

21. Nikolsky BP. Spravochnik khimika. Tom 3 [Chemist's handbook. Volume 3]. Leningrad: Khimiya; 1971. 1008 p. Russian.

22. Rietveld HM. A profile refinement method for nuclear and magnetic structures. J Appl Crystallogr. 1969;2(2):65–71. doi:10.1107/S0021889869006558

23. Bush DL, Post JE. A survey of using programs for the Rietveld profile refinement. Reviews in mineralogy. 1990;20:369–74. doi:10.1180/claymin.1990.025.4.12

24. Rodriges-Carvajal J. Recent advances in magnetic structure determination by neutron powder diffraction. Physica B. 1993;192:55–69. doi:10.1016/0921-4526(93)90108-I

25. Williamson GK, Hall WH. X-ray line broadening from filed aluminium and wolfram. Acta Metall. 1953;1:22–31. doi:10.1016/0001-6160(53)90006-6

26. Maskaeva LN, Markov VF, Vaganova IV, et al. Films of supersaturated $Cd_xPb_{1-x}S$ solid solutions: composition prognostication, chemical synthesis, microstructure. Russ J Appl Chem. 2017;90(5):691–700. doi:10.1134/S1070427217050044

27. Vinogradova TV, Markov VF, Maskaeva LN. Temperature dependence of constants of thiourea hydrolytic decomposition and cyanamide. Stepwise ionization. Russ J Gen Chem. 2010;80:2341–6. doi:10.1134/S1070363210110198

28. Maskaeva LN, Markov VF, Forostyanaya NA, et al. Kinetic aspects of hydrochemical deposition of cadmium sulfide from solutions with diverse ligand backgrounds. Russ J Gen Chem. 2016;86(10):2273–81. doi:10.1134/S1070363216100054

29. Lee S-M, Cho S-N, Cheon J. Anisotropic shape control of colloidal inorganic nanocrystals. Adv Mater. 2003;15(5):441–4. doi:10.1002/adma.200390102

30. Forostyanaya NA, Maskaeva LN, Markov VF. Influence of the ligand nature on the boundary conditions of the formation and the morphology of nanocrystalline cadmium sulfide films. Russ J Gen Chem. 2015;85:2513–19. doi:10.1134/S1070363215110031

31. Markov VF, Maskaeva LN. Nucleation and mechanism of metal sulfide film growth using deposition by thiocarbamide. Russ Chem Bull. 2014;63(7):1523–32. doi:10.1007/s11172-014-0630-7

32. Bugaenko LT, Ryabykh SM, Bugaenko AL. A nearly complete system of average crystallographic ionic radii and its use for determining ionization potentials. Moscow Univ Chem Bull. 2008;63:303–17. doi:10.3103/S0027131408060011

33. Kobayashi T, Susa K, Taniguchi S. Preparation and semiconductive properties of rock salt type solid solution systems, $Cd_{1-x}M_xS$ (M = Sr, Ca, Mg, Pb, Sn). J Phys Chem Solids. 1979;40:781–5. doi:10.1016/0022-3697(79)90160-4

34. Corll JA. Recovery of the high-pressure phase of cadmium sulfide. J Appl Phys. 1964;35(10):3032–3. doi:10.1063/1.1713151

35. Rooymans CJM. Structure of the high pressure phase of CdS, CdSe, and InSb. Phys Lett. 1963;4:186–7. doi:10.1016/0031-9163(63)90356-1

36. Susa K, Kobayashi T, Taniguchi S. High-pressure synthesis of rock-salt type CdS using metal sulfide additives. J Solid State Chem. 1980;33:197–202. doi:10.1016/0022-4596(80)90120-6

37. Vegard L. Die konstitution der mischkristalle und die raumfüllung der atome. Zeitschrift für Physik. 1921;5:17–26. doi:10.1007/BF01349680

38. Denton AR, Ashcroft NW. Vegard's law. Phys Rev A. 1991;43:3161–4. doi:10.1103/PhysRevA.43.3161

39. Shelimova LE, Tomashik VN, Gritsyv VI. Diagrammy sostoyaniya v poluprovodnikovom materialakh (sistemy na osnove khal'kogenidov Si, Ge, Sn, Pb) [State diagrams in semiconductor materials science (systems based on chalcogenides Si, Ge, Sn, Pb]. Moscow: Nauka; 1991. 368 p. Russian.